Design of a cosine pulse transceiver operating in the discrete-time domain

Stevan M. Berber
The University of Auckland,
Department of Electrical, Computer and Software Engineering,
Auckland, New Zealand,
e-mail: s.berber@auckland.ac.nz,
ORCID ID: https://orcid.org/0000-0002-2432-3088

DOI: 10.5937/vojtehg71-43566; https://doi.org/10.5937/vojtehg71-43566

FIELD: electrical engineering, telecommunications
ARTICLE TYPE: original scientific paper

Abstract:

Introduction/purpose: The paper presents the theory and the design issues of a transceiver for a discrete-time cosine pulse transmission. The operation of the transceiver and all signals are analyzed in both time and frequency domains.

Methods: The detailed theoretical models of the transmitter and the receiver are presented based on their block schematics expressed in terms of mathematical operators. The transceiver blocks are simulated and the results of their simulation are presented and compared with the theoretical results.

Results: Discrete-time signals at the input and the output of each transceiver block are derived in the mathematical form and presented in the time and frequency domain. A transceiver simulator is developed in Matlab. The simulation results confirmed the theoretical findings.

Conclusion: The results of this work contribute to the theoretical modeling and design of modern transceivers that can be used for discrete-time cosine pulse transmission.

Keywords: transceiver design, discrete cosine pulse, pulse transceiver, transceiver mathematical modeling, filtering, transceiver simulation.

Introduction

Designs of communication transmitters and receivers are based on the presentation of signals in the continuous-time domain, i.e., in their analysis and synthesis, signals are presented as continuous functions of time. Related communication systems, composed of these devices, are known under the name of digital communication systems (Haykin, 2014; Proakis, 2001). Due to the development of advanced digital technology, signals of modern communication systems are represented by discrete-

time functions and are known under the name discrete communication systems (Rice, 2009; Berber, 2021; Abramowitz & Stegun, 1972).

Designs of modern transmitters and receivers are implemented in digital technology, primarily on FPGA and DSP platforms. Using these technologies, the signal processing operations inside both baseband and intermediate frequency transceiver blocks are implemented using the signal presentation in the discrete-time domain. These designs became possible due to the advances in the mathematical theory of discrete-time signal processing, and, in particular, due to the development of the mathematical theory of discrete-time deterministic and stochastic processes (Manolakis et al, 2005; Berber, 2009).

This paper presents the theoretical base of a discrete communication system assuming that the modulating signal is a cosine discrete-time pulse, including the issues of mathematical modeling and design of a discrete communication system composed of a transmitter, a transmission channel, and a receiver. The signals are expressed as functions of the discrete-time variables. To distinguish discrete systems from digital systems, we named systems operating in the continuous time domain digital systems, and systems operating in the discrete-time domain we named *discrete systems* (Miao, 2007; Benvenuto et al, 2007; Berber, 2021).

In particular, the structure and the operation of the receiver having a low-pass filter at the receiver side are analyzed. The presented system structures are expressed in terms of mathematical operators and their operations are explained using exact mathematical expressions. The designed transceiver is simulated to confirm the presented mathematical model (Ingle & Proakis, 2012; Nguyen et al, 2015).

Based on the time and frequency domain presentation of the transceiver signals, and the power and energy spectral densities calculations, the power and the energies of the related signals are calculated assuming the ideal transmission of the signals in the noiseless channel. These calculations allowed a clear understanding of the transceiver operation and the estimations of possible losses in signal powers that were caused by the signal processing in the transceiver.

The presented theory of modern discrete communication systems design is of vital importance for researchers, practicing engineers, and designers of transceiver devices because the design of these devices is impossible without a deep understanding of the theoretical principles and concepts related to their operation in the discrete-time domain (Rice, 2009; Berber, 2021).

Discrete-time communication system structure and operation

A block schematic of a discrete communication system under consideration, which includes its basic block presented in the form of mathematical operators, is shown in Figure 1. The system consists of a transmitter, a band-pass noise generator, and a receiver. At the input of the transmitter there is a low frequency (LF) discrete rectangular pulse $p(n)$ that modulates an LF cosine signal $s_m(n)$ to produce an LF cosine pulse $m(n)$. This cosine pulse modulates the carrier $s_c(n)$. The obtained band-pass modulated signal $s(n)$ is generated at the output of the transmitter.

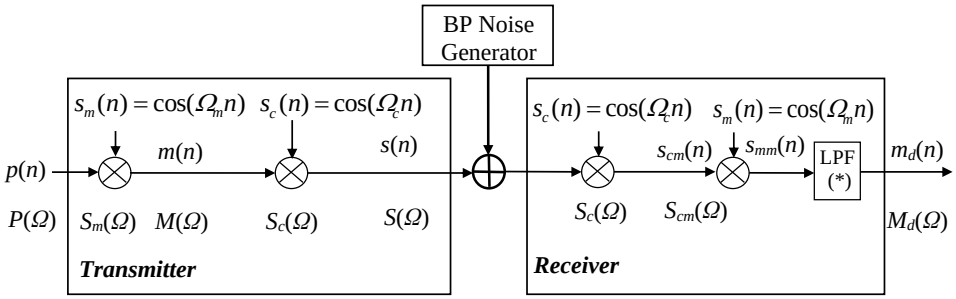

Figure 1 – Block schematic of a communication system operating in the discrete-time domain
Рис. 1 – Структурная схема системы связи, работающей в области дискретного времени
Слика 1 – Блок-шема комуникационог система који ради у домену дискретног времена

The coherent receiver will demodulate the received band-pass (BP) signal using a low-pass filter (LPF) and generate an estimate of the cosine pulse or the rectangular pulse transmitted. Firstly, the modulated signal $s(n)$ is multiplied by the carrier $s_c(n)$ to obtain the demodulated cosine pulse $s_{cm}(n)$. Then, the cosine pulse is multiplied by the LF cosine signal $s_m(n)$ to obtain a signal $s_{mm}(n)$ that contains the rectangular pulse that can be extracted by the low-pass filter (LPF). In the case of the system simulation, a band-pass noise generator should be used to investigate the operation of the system in real conditions. Because the system operates with discrete-time signals, the noise generator needs to generate a BP discrete-time noise that will be added to the modulated discrete-time signal.

Transmitter operation

We will generate the discrete-time cosine pulse and then modulate the carrier with that cosine pulse. The block schematic of the transmitter is presented in Figure 1. The generated pulse can be considered an LF cosine pulse. However, our question is how to generate the band-pass sinusoidal pulse with the modulating signal that is this LF cosine signal. For that purpose, as we expect, the carrier frequency should be much higher than the bandwidth of the LF cosine pulse. Let us assume, for the sake of explanation and presentation, that the carrier frequency is 10 times higher than the middle frequency of the LF cosine pulse.

To generate this modulated pulse, we need to multiply the LF cosine pulse with the carrier, as shown in Figure 1. The carrier frequency is 10 times higher than the frequency of the cosine pulse, i.e., $f_c = 10f_m$. Suppose the minimum number of samples in one period of the carrier is $N_c = 4$. Therefore, the number of samples N of the rectangular pulse $p(n)$ (for 2 oscillations of the LF cosine pulse and 20 oscillations of the carrier and the number of samples N_m in one period of the LF cosine signal) needs to be calculated to accommodate the 10 times higher frequency of the carrier, i.e.,

$$N = 10 \cdot 2 \cdot N_c = 20 \cdot 4 = 80. \quad (1)$$

The number of samples inside one period of the LF cosine pulse now is calculated to be $N_m = N/2 = 40$. Therefore, to perform the multiplication of the rectangular pulse by the LF cosine signal and then modulate the carrier, the number of their samples should be 80. The mathematical expressions and related wave shapes of the transmitter signals will be presented in the following analysis. For the calculated values of the discrete signals, we can analyze their properties in the time and frequency domain at each block of the transceiver.

The rectangular pulse presentation in the time and frequency domain. Based on the calculated number of samples inside the processed signals, the graphs of the discrete-time (dt) rectangular pulse $p(n)$ in the discrete-time domain are presented in Figure 2. The signal is expressed in terms of the Kronecker delta functions as a convolution of the signal and the delta functions. i.e.,

$$p(n) = \sum_{k=0}^{N-1} m(k)\delta(n-k) = \begin{Bmatrix} A & 0 \le n \le N-1 \\ 0 & otherwise \end{Bmatrix} = \begin{Bmatrix} A & 0 \le n \le 79 \\ 0 & otherwise \end{Bmatrix}. \quad (2)$$

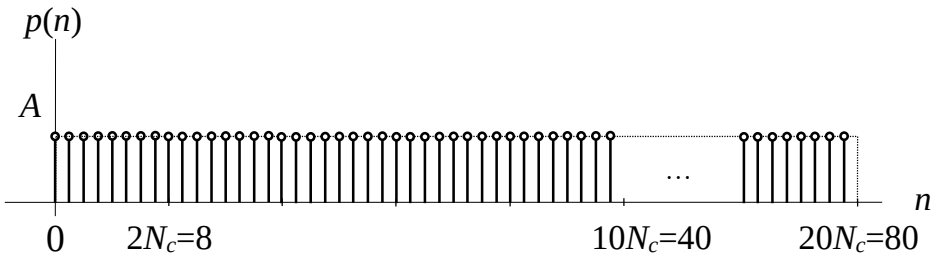

Figure 2 − Discrete-time modulating signal for N = 80 and A = 2
Рис. 2 – Модулирующий сигнал с дискретным временем при N = 80 и A = 2
Слика 2 – Модулишући сигнал дискретног времена за N = 80 и A = 2

It is to note that the discrete-time pulse values are defined for each whole number n and have no values in the intervals between neighboring numbers. We can say that the signal values do not exist in these intervals, even though these intervals are used to process the discrete signal values. The related magnitude and phase spectral densities can be obtained from the DTFT of the dt rectangular pulse which is defined as

$$P(\Omega)=\sum_{n=-\infty}^{\infty}p(n)e^{-j\Omega n}=\sum_{n=0}^{n=(N-1)}Ae^{-j\Omega n}$$

$$=\left\{\begin{array}{cc} AN & \Omega=\pm 2k\pi, k=0,1,2,3,... \\ Ae^{-j\Omega(N-1)/2}\dfrac{\sin(\Omega N/2)}{\sin(\Omega/2)} & \text{otherwise} \end{array}\right\}\Big| N=80 \quad , (3)$$

and is to be calculated for N = 80. The magnitude spectral density can be expressed as

$$P(\Omega)=\left\{\begin{array}{cc} |AN| & \Omega=\pm 2k\pi, k=0,1,2,3,... \\ \left|A\dfrac{\sin(\Omega N/2)}{\sin(\Omega/2)}\right| & otherwise \end{array}\right\}, \qquad (4)$$

which is graphically presented in Figure 3 for the defined duration of the pulse N = 80 and the amplitude A = 2. The zeros in the magnitude spectrum occur for the condition expressed as $\sin(\Omega_0 N/2)=0$, i.e., for $\Omega_0 N/2 = k\pi$ or k = 1, 2, …, N-1. For N = 80, we may have $\Omega_0 = \pm 2k\pi/N = \pm k\pi/40$, and k = 1, 2, …, 79. The phase discontinuities of π radians occur at the same frequencies. The related magnitude spectral density is shown in Figure 3.

Berber, S., Design of a cosine pulse transceiver operating in the discrete-time domain, pp.559-587

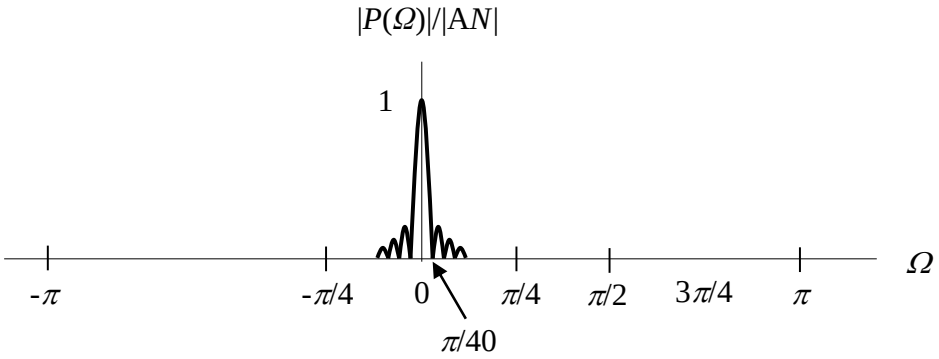

Figure 3 − Magnitude spectral density of the rectangular pulse
Рис. 3 – Спектральная плотность колебаний правоугольного импульса
Слика 3 – Спектрална густина магнитуде правоугаоног пулса

The first zero crossing occurs at the frequency $\pi/40$. The magnitude value for zero frequency is normalized by $|AN|$ to be one. We can calculate the power and energy of the pulse in the time domain for the values of the signal that are different from zero as

$$P_p = \frac{1}{N}\sum_{n=0}^{N-1} p^2(n) = \frac{1}{80}\sum_{n=0}^{n=79} A^2 = \frac{1}{80}80A^2 = A^2, \tag{5}$$

$$E_p = P_p \cdot N = \sum_{n=0}^{N-1} p^2(n) = \sum_{n=0}^{n=79} A^2 = NA^2 = 80A^2. \tag{6}$$

On the other hand, the energy spectral density (ESD) of the pulse is defined as the magnitude spectral density square and expressed as

$$E_p(\Omega) = \left|P(\Omega)\right|^2 = \left|A\frac{\sin(\Omega N/2)}{\sin(\Omega/2)}\right|^2. \tag{7}$$

In the frequency domain, the energy of the pulse is calculated as an integral of the ESD in this way (Integral calculator, 2023)

$$E_p = \frac{1}{2\pi}\int_{-\pi}^{\pi}\left|P(\Omega)\right|^2 d\Omega = \frac{A^2}{2\pi}\int_{-\pi}^{\pi}\left|\frac{\sin(\Omega N/2)}{\sin(\Omega/2)}\right|^2 d\Omega = \frac{A^2}{2\pi}160\pi = NA^2 = 80A^2. \tag{8}$$

The ESD can be calculated also as the DTFT of the autocorrelation function of the discrete rectangular pulse (Berber, 2019, 2021).

*The LF cosine signal in the time and frequency domain***.** The LF cosine signal has N_m = 40 samples per oscillation, which can be understood as a subcarrier in the system. Therefore, its frequency is $\Omega_m = 2\pi f_m / f_s = 2\pi / N_m = \pi / 20$. This signal in the time domain is

$$s_m(n) = \cos \Omega_m n = \cos 2\pi n / N_m = \cos \pi n / 20 , \quad (9)$$

which is shown in a graphical form in Figure 4a).

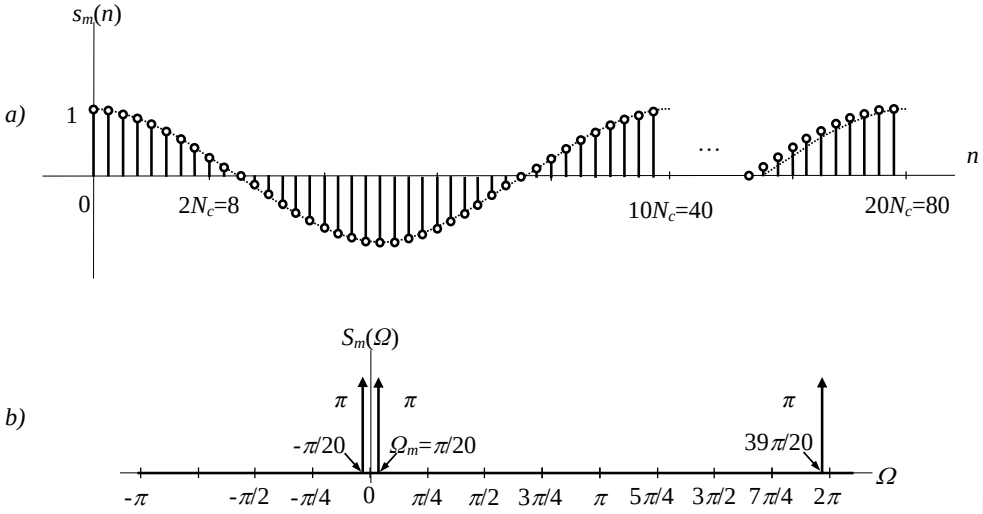

Figure 4 − a) Waveshape of the LF sinusoid signal, b) related amplitude spectral density
Рис. 4 – а) Форма волны низкочастотного синусоидального сигнала, б) соответствующая амплитудная спектральная плотность
Слика 4 – а) Таласни облик НФ синусоидалног сигнала, б) односна спектрална густина амплитуде

The signal in the frequency domain can be directly found for any N_m simply applying Euler's formula on the time domain as follows

$$s_m(n) = \frac{1}{2}[e^{j2\pi n/N_m} + e^{j2\pi n(N_m-1)/N_m}] = \frac{1}{2}(e^{j\pi n/20} + e^{j\pi n 39/20}) , \quad (10)$$

or the amplitude spectral density expressed as

$$S_m(\Omega) = \sum_{k=\pm 1} \frac{2\pi}{2} \delta(\Omega + k \cdot \Omega_m) = \pi\delta(\Omega + \Omega_m) + \pi\delta(\Omega - \Omega_m) , \quad (11)$$

which is a periodic function of the continuous frequency Ω with the period of 2π, as presented in Figure 4b). This spectrum can be represented by a periodic stream of the Dirac delta functions (Papoulis & Pillai, 2002) weighting π at periodic frequencies and zeros everywhere else.

The power of the signal in the time domain is calculated as

$$P_{sm} = \frac{1}{N_m}\sum_{n=0}^{N_m-1}\cos^2(\Omega_m n) = \frac{1}{40}\sum_{n=0}^{39}\cos^2(\pi n/2) = \frac{1}{40}\sum_{n=0}^{39}\frac{1}{2} = \frac{1}{2}. \quad (12)$$

This is a power signal (Cavicchi, 2007; Berber, 2021). Therefore, its average power is to be calculated in the infinite interval, according to this expression

$$P_{sm} = \lim_{a\to\infty}\frac{1}{2a}\sum_{n=-a}^{a}\cos^2(\Omega_m n) = \lim_{a\to\infty}\frac{1}{2a}\sum_{n=-a}^{a}\frac{1}{2}(1+\cos\pi n/2) = \lim_{a\to\infty}\frac{1}{2a}\frac{2a}{2} = \frac{1}{2}. \quad (13)$$

Because this signal in the frequency domain is a periodic function of the continuous frequency Ω with a period of 2π, it can be represented by a periodic stream of the Dirac delta functions, as presented in Figure 4b). The energy of the signal is

$$E_{sm} = \frac{1}{2\pi}\int_{-\infty}^{\infty}|S_m^2(\Omega)|\,d\Omega = \frac{1}{2\pi}\int_{-\pi}^{\pi}\left(\sum_{k=\pm1}\frac{2\pi}{2}\delta(\Omega+k\Omega_m)\right)^2 d\Omega$$

$$= \frac{\pi}{2}\int_{-\pi}^{\pi}\left(\delta^2(\Omega+\Omega_m)+2\delta(\Omega+\Omega_m)\delta(\Omega-\Omega_m)+\delta^2(\Omega-\Omega_m)\right)d\Omega. \quad (14)$$

$$\to\infty+0+\infty\to\infty$$

The infinite energy value can be confirmed by its calculation in the time domain as

$$E_{sm} = \lim_{a\to\infty}\sum_{n=-a}^{a}\cos^2(\Omega_m n) = \lim_{a\to\infty}\sum_{n=-a}^{a}\frac{1}{2}(1+\cos\pi n/2) = \lim_{a\to\infty}\frac{2a}{2} = \infty. \quad (15)$$

The LF cosine pulse in the time and frequency domain. The cosine pulse $m(n)$ is obtained by multiplying the $s_m(n)$ shown in Figure 1 by the rectangular pulse $p(n)$. This is again a cosine function. However, it is not a periodic function as it was the LF cosine signal $s_m(n)$. Consequently, it will not be expressed in the frequency domain in terms of the Dirac delta functions. Instead of one spectral component, the spectrum of the cosine pulse will have a bandwidth around the frequency of the periodic cosine signal. The cosine pulse can be expressed in the time domain as

$$m(n) = p(n)s_m(n) = \begin{Bmatrix} A\cos\Omega_m n & 0 \le n \le N-1 \\ 0 & otherwise \end{Bmatrix} = \begin{Bmatrix} A\cos\pi n/20 & 0 \le n \le 79 \\ 0 & otherwise \end{Bmatrix}, \quad (16)$$

and, based on the modulation theorem, in the frequency domain as

$$M(\Omega) = FT\{p(n)\cos\Omega_m n\} = \frac{1}{2}[P(\Omega-\Omega_m) + P(\Omega+\Omega_m)], \quad (17)$$

where its shifted components are expressed as

$$\frac{1}{2}P(\Omega\pm\Omega_m) = \begin{Bmatrix} AN/2 & \Omega\pm\Omega_m = \mp 2k\pi, k = 0, 1, ... \\ \frac{A}{2}e^{-j(\Omega\pm\Omega_m)(N-1)/2}\frac{\sin((\Omega\pm\Omega_m)N/2)}{\sin((\Omega\pm\Omega_m)/2)} & \text{otherwise} \end{Bmatrix}$$

The cosine pulse and the related magnitude spectral density are presented in Figure 5.

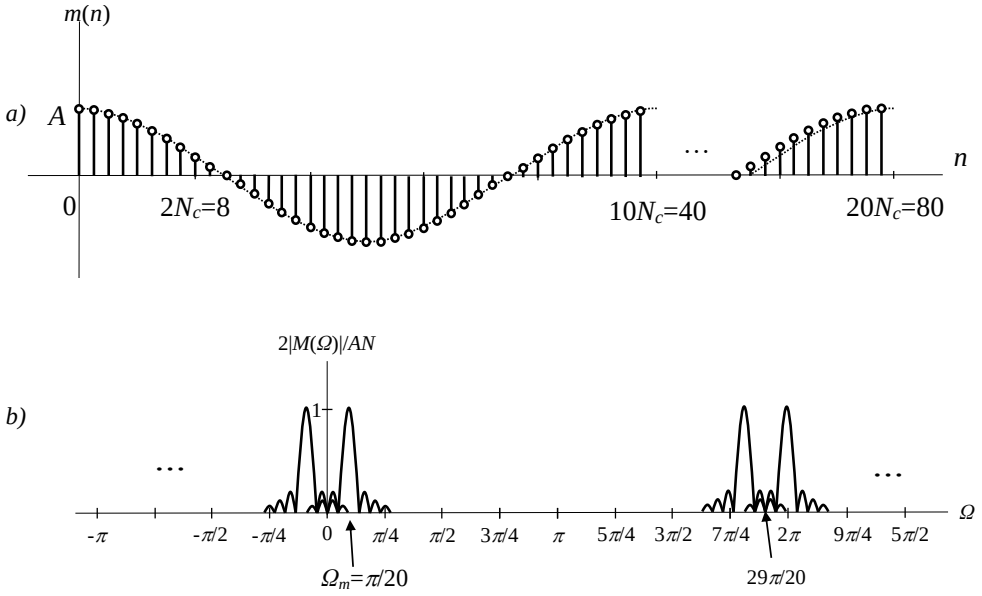

Figure 5 – a) Pulse in the time domain, b) Magnitude spectral density of the pulse
Рис. 5 – a) *Форма импульса во временной области б) спектральная плотность амплитуды импульса*
Слика 5 – а) Таласни облик пулса у временском домену, б) спектрална густина магнитуде пулса

The power and the energy of the cosine LF pulse are

$$P_m = \frac{1}{N}\sum_{n=0}^{N-1} A^2\cos^2(\Omega_m n) = \frac{1}{80}\sum_{n=0}^{n=79}\frac{1}{2}A^2(1+\cos\pi n) = \frac{A^2}{80}\sum_{n=0}^{n=79}\frac{1}{2} = \frac{A^2}{2}, \quad (18)$$

$$E_m = NP_m = \sum_{n=0}^{N-1} A^2\cos^2(\Omega_m n) = 40A^2. \quad (19)$$

The amplitude spectral density is a periodic function of continuous frequency with the period of 2π as presented in Figure 5b). The signal is an energy signal, and its energy can be calculated from the energy spectral density (Integral calculator, 2023) as

$$E_m = \frac{1}{2\pi}\int_{-\pi}^{\pi}\left|M(\Omega)\right|^2 d\Omega = \frac{1}{8\pi}\int_{-\pi}^{\pi}\left|P(\Omega-\Omega_m)+P(\Omega+\Omega_m)\right|^2 d\Omega = \frac{A^2}{8\pi}2\cdot 160\pi = 40A^2 \quad (20)$$

The carrier in the time and frequency domain. For the defined frequency, the carrier of a unit amplitude is expressed in the discrete-time domain as

$$s_c(n) = \cos\Omega_c n = \cos 2\pi n / N_c = \cos\pi n/2 \quad (21)$$

as presented in Figure 6a). The carrier in the frequency domain can be directly found, for the number of samples $N_c = 4$ in one period of the carrier, by simply applying Euler's formula on the time domain expression of the signal and we may have

$$S_c(\Omega) = \sum_{k=\pm 1}\frac{2\pi}{2}\delta(\Omega+k\cdot\Omega_c) = \pi\delta(\Omega+\Omega_c)+\pi\delta(\Omega-\Omega_c), \quad (22)$$

which is a periodic function of frequency with the period of 2π, as presented in Figure 6b). Because this signal is a periodic function of the continuous frequency Ω with a period of 2π, it is represented by a periodic stream of the Dirac delta functions (Papoulis & Pillai, 2002), as presented in Figure 6b).

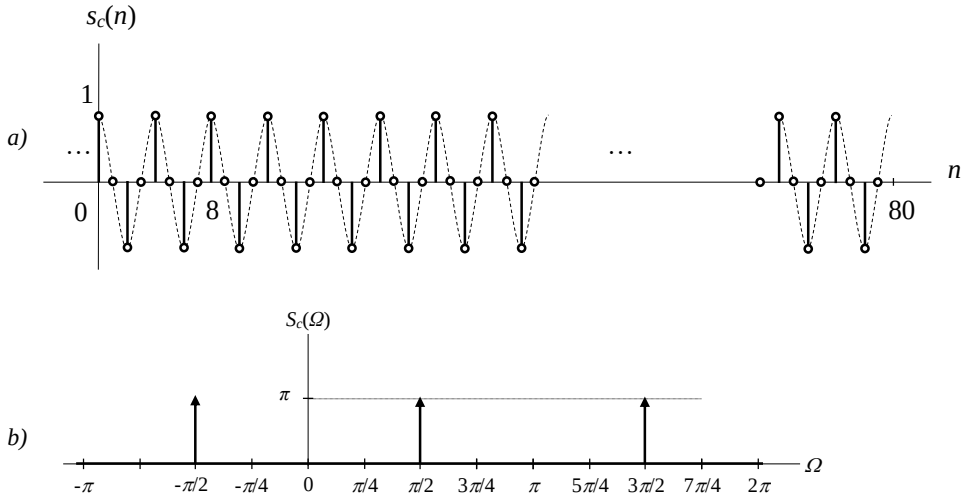

Figure 6 – a) Carrier in the time domain, b) Magnitude spectral density of the carrier
Рис. 6 – а) *Несущая волна во временной области, б) спектральная плотность колебаний несущей волны*
Слика 6 – а) Носилац у временском домену, б) спектрална густина амплитуде носиоца

The modulated signal in the time and frequency domain. The modulated signal $s(n)$ is obtained by multiplying the LF cosine pulse $m(n)$ by the carrier $s_c(n)$. The LF signal $m(n)$ is obtained by multiplying the signals $s_m(n)$ by the rectangular pulse $p(n)$, as shown in Figure 5a). Therefore, the modulated signal in the time domain is expressed as

$$s(n) = m(n) \cdot s_c(n) = p(n) s_m(n) \cdot \cos \Omega_c n \,, \qquad (23)$$

and presented in Figure 7a). By applying the modulation property of DTFT, we may get the amplitude spectral density of that signal as

$$S(\Omega) = FT\{m(n)\cos \Omega_c n\} = \frac{1}{2} FT\left\{m(n)(e^{j\Omega_c n} + e^{-j\Omega_c n})\right\} = \frac{1}{2}[M(\Omega - \Omega_c) + M(\Omega + \Omega_c)] \,. \qquad (24)$$

We can find its shifted components in (24) and express them as

$$\frac{1}{2}M\left(\Omega\pm\Omega_c\right)=\frac{A}{2}e^{-j(\Omega-\Omega_c)(N-1)/2}\frac{\sin\left((\Omega\pm\Omega_c)N/2\right)}{\sin\left((\Omega\pm\Omega_c)/2\right)}$$

$$=\begin{cases} AN/2 & \Omega\pm\Omega_c=\mp 2k\pi, k=0,1,2,3,... \\ \frac{A}{2}e^{-j(\Omega\pm\Omega_c)(N-1)/2}\frac{\sin\left((\Omega\pm\Omega_c)N/2\right)}{\sin\left((\Omega\pm\Omega_c)/2\right)} & otherwise \end{cases},$$

where N = 80 for our case. Then, based on expression (17) for the amplitude spectral density of $m(n)$, the magnitude spectral density of the modulated signal (24) finally is

$$S(\Omega)=\frac{1}{4}[P(\Omega-\Omega_c-\Omega_m)+P(\Omega-\Omega_c+\Omega_m)] + \frac{1}{4}[P(\Omega+\Omega_c-\Omega_m)+P(\Omega+\Omega_c+\Omega_m)] \quad (25)$$

For the defined values of frequency $\Omega_m=\pi/20$ and $\Omega_c=\pi/2$, the magnitude spectral density of the modulated signal is presented in Figure 7b).

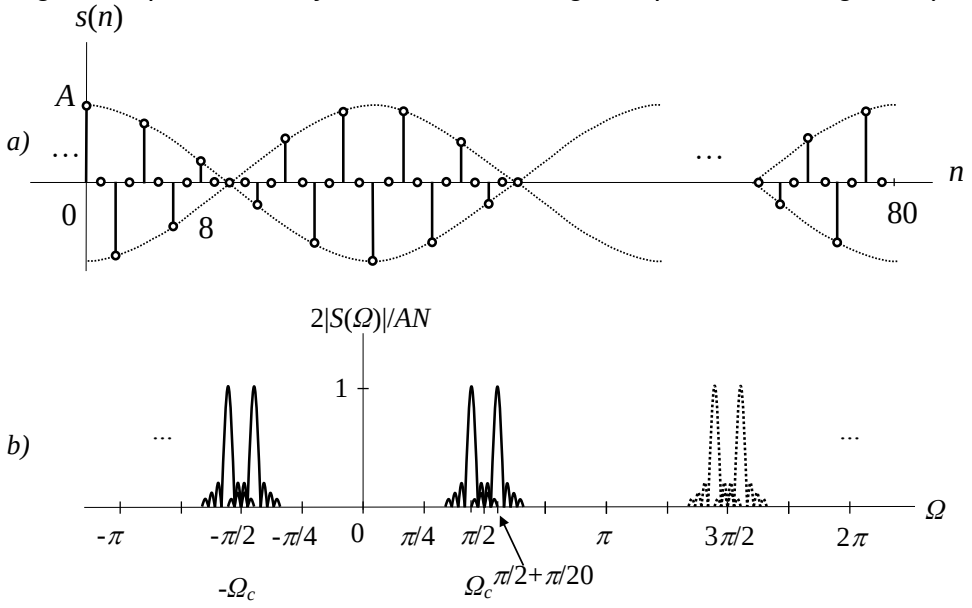

Figure 7 – a) Modulated signal in the time domain, and b) in the frequency domain
Рис. 7 – а) Модулированный сигнал во временной области и б) в частотной области
Слика 7 – а) Модулисани сигнал у временском домену, и б) у фреквенцијском домену

The magnitude spectrum is a periodic function with a period of 2π. The two-sided spectrum of the signal can be investigated inside the bandwidth around the carrier frequency of $\pi/2$.

The power of the modulated signal can be calculated in the time domain as

$$P_s = \frac{1}{N}\sum_{n=0}^{N-1} s^2(n) = \frac{1}{N}\sum_{n=0}^{N-1} p^2(n)\cos^2(\Omega_m n)\cdot\cos^2\Omega_c n$$
$$= \frac{A^2}{320}\sum_{n=0}^{n=79}(1+\cos 2\Omega_m n)\cdot(1+\cos 2\Omega_c n) = \frac{A^2}{320}\sum_{n=0}^{n=79} 1 = \frac{A^2}{4} \quad (26)$$

The energy of the signal, based on solution (20), is

$$E_s = P_s N = \frac{1}{2\pi}\int_{-\pi}^{\pi} \left|S(\Omega)\right|^2 d\Omega$$
$$= \frac{A^2}{4}\frac{1}{2\pi}\int_{-\pi}^{\pi} \left|M(\Omega-\Omega_c)+M(\Omega+\Omega_c)\right|^2 d\Omega = \frac{A^2}{4}(40+40) = 20A^2 \quad (27)$$

which can be calculated as shown before. From the energy expression, it is easy to find the power of the signal and vice versa.

Simulation of the transmitter operation

We performed a simulation in Matlab of the transmitter presented in Figure 1 (Ingle & Proakis, 2012). The signals are generated in the time and frequency domain and presented in graphical forms. The modulating signal obtained by simulation in the time and frequency domain is presented in Figure 8. They are equivalent to the signals that have been obtained by calculations and presented in Figures 2 and 3, respectively.

The pulse $p(n)$ is presented by all 800 values of amplitude for the sake of illustrating what the part of the signal where amplitudes greater than zero looks like. A theoretically expected graph of this signal in the time domain is shown in Figure 2.

A simulated LF cosine signal is presented in the time and frequency domain in Figure 9**.** The signal in the time domain has N_m = 40 samples per oscillation. That signal in the time domain is presented in Figure 9. The signal in the frequency domain contains only two components in the bandwidth from $-\pi$ to $+\pi$. This is a periodic function of frequency. Theoretically expected graphs of this signal are shown in Figure 4.

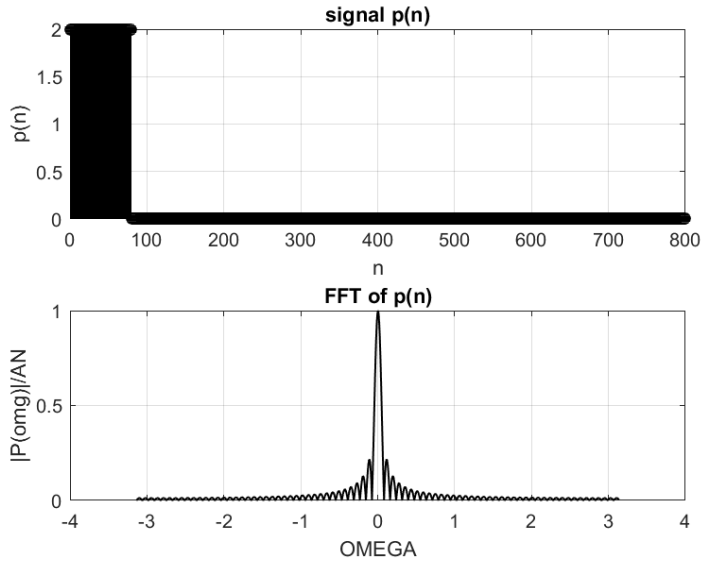

Figure 8 – Modulating signal in the time and frequency domain
Рис. 8 – Модулирующий сигнал во временной и частотной областях
Слика 8 – Модулишући сигнал у временском и фреквенцијском домену

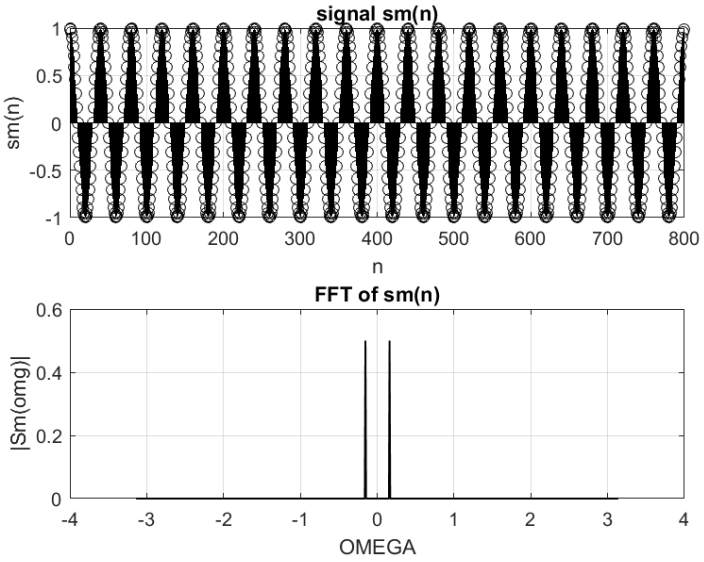

Figure 9 – The LF cosine signal in the time and frequency domain
Рис. 9 – Низкочастотный косинусоидальный сигнал во временной и частотной областях
Слика 9 – НФ косинусни сигнал у временском и фреквенцијском домену

A simulated LF cosine pulse in the time and frequency domain is shown in Figure 10. The cosine pulse $m(n)$ has the amplitudes $A = 2$ in the interval from $n = 0$ to $n = 80$. It is not a periodic function, and its spectrum is a shifted version of the spectrum of the rectangular pulse to the frequency Ω_m. The graphs in Figure 10 correspond to the theoretical graphs shown in Figure 5.

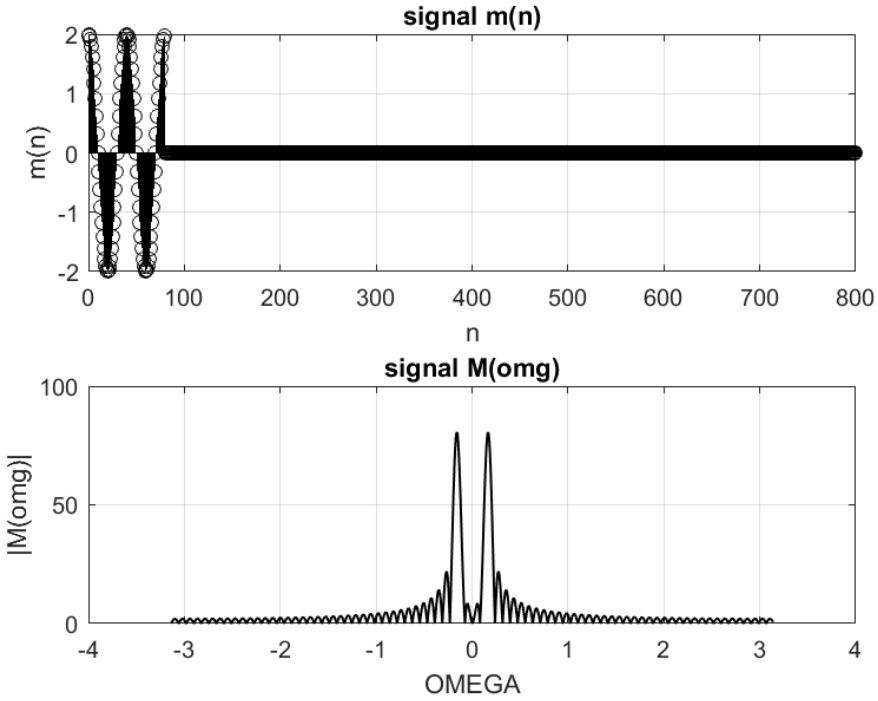

Figure 10 – LF cosine pulse in the time and frequency domain
Рис. 10 – Низкочастотный косинусоидальный сигнал во временной и частотной областях
Слика 10 – НФ косинусни пулс у временском и фреквенцијском домену

The simulated high-frequency carrier is shown in the time and frequency domain in Figure 11. The processed carrier was in the interval from $n = 0$ to $n = 800$. In Figure 11, only a part of the signal is shown for the sake of understanding its shape. These graphs correspond to the theoretically expected graphs presented in Figure 6.

The simulated modulated signal in the time and frequency domain is presented in Figure 12. The same signal in the time domain is presented in an extended form in Figure 13. These graphs correspond to the theoretically expected graphs presented in Figure 7.

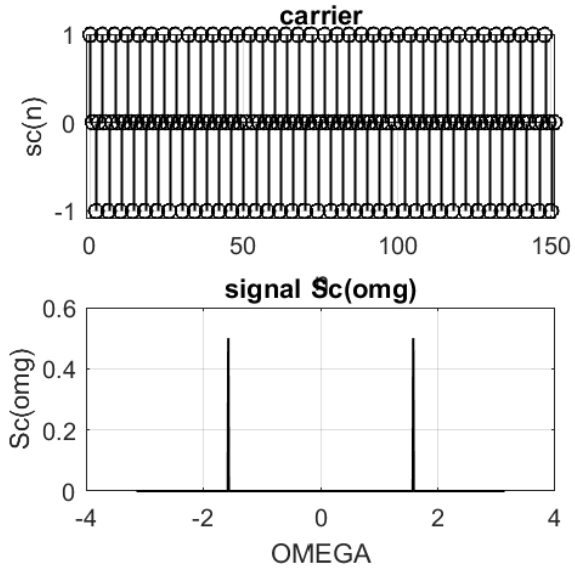

Figure 11 – The carrier signal in the time and frequency domain
Рис. 11 – Несущая волна во временной и частотной областях
Слика 11 – Носилац у временском и фреквенцијском домену

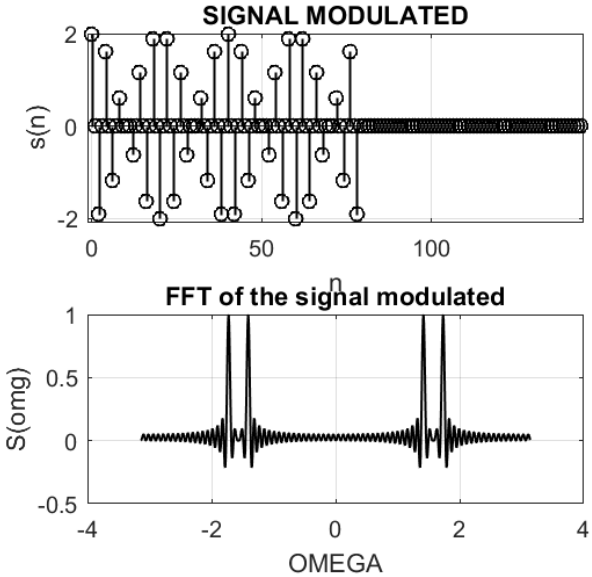

Figure 12 – Modulated signal in the time and frequency domain
Рис. 12 – Модулированный сигнал во временной и частотной областях
Слика 12 – Модулисани сигнал у временском и фреквенцијском домену

To see the shape of the signal, the modulated signal $s(n)$ is presented in the whole interval from $n = 0$ to $n = N$-1 in Figure 13.

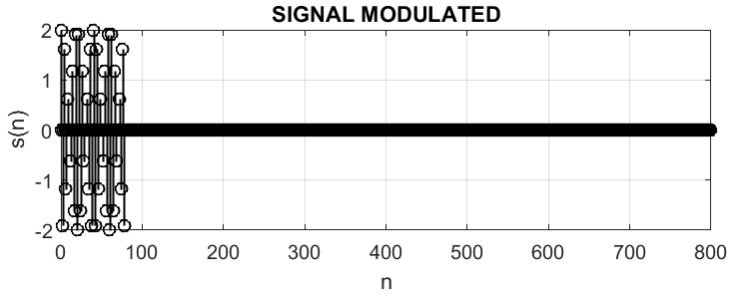

Figure 13 – Modulated signal in the time domain
Рис. 13 – Модулированный сигнал во временной области
Слика 13 – Модулисани сигнал у временском домену

Pulse demodulator

The demodulation of the discrete modulated signal $s(n)$ results in the discovery of the modulating cosine and the rectangular pulse. The receiver blocks involved in the procedure of received signal demodulation are presented in Figure 1.

The output signal of the demodulator multiplier. Firstly, the received discrete modulated signal is multiplied by the carrier to get the signal

$$s_{cm}(n) = s(n)\cos\Omega_c n = \begin{Bmatrix} m(n)\cos^2\Omega_c n & 0 \le n \le N-1 \\ 0 & otherwise \end{Bmatrix}$$

$$= \begin{Bmatrix} \frac{1}{2}m(n)(1+\cos 2\Omega_c n) & 0 \le n \le N-1 \\ 0 & otherwise \end{Bmatrix} . \quad (28)$$

The signal can be expressed in this form in the time domain

$$s_{cm}(n) = \begin{Bmatrix} \frac{1}{2}A\cos\Omega_m n + \frac{1}{2}\frac{1}{2}A\cos(2\Omega_c + \Omega_m)n + \frac{1}{2}\frac{1}{2}A\cos(2\Omega_c - \Omega_m)n & 0 \le n \le N-1 \\ 0 & otherwise \end{Bmatrix} \quad (29)$$

Therefore, the DTFT of this signal gives us its amplitude spectral density expressed as

$$S_{cm}(\Omega) = \frac{1}{2}FT\{m(n)(1+\cos 2\Omega_c n)\} = \frac{1}{2}FT\{m(n) + m(n)\cos 2\Omega_c n\}$$
$$= \frac{1}{2}M(\Omega) + \frac{1}{4}[M(\Omega - 2\Omega_c) + M(\Omega + 2\Omega_c)] , \quad (30)$$

where the first component $M(\Omega)$ is the LF component containing the spectrum of the modulating cosine pulse and its shifted spectrum to the doubled carrier frequency. The LF component can be expressed as

$$\frac{1}{2}M(\Omega)=\frac{1}{2}FT\{p(n)\cos\Omega_m n\}=\frac{1}{4}[P(\Omega-\Omega_m)+P(\Omega+\Omega_m)], \quad (31)$$

where the shifted components are

$$P(\Omega-\Omega_m)=\left\{\begin{array}{ll} AN & \Omega-\Omega_m=\pm 2k\pi, k=0,1,2,3,... \\ Ae^{-j(\Omega-\Omega_m)(N-1)/2}\dfrac{\sin((\Omega-\Omega_m)N/2)}{\sin((\Omega-\Omega_m)/2)} & \text{otherwise} \end{array}\right\}\Bigg|_{N=80}$$

$$P(\Omega+\Omega_m)=\left\{\begin{array}{ll} AN & \Omega+\Omega_m=\pm 2k\pi, k=0,1,2,3,... \\ Ae^{-j(\Omega+\Omega_m)(N-1)/2}\dfrac{\sin((\Omega+\Omega_m)N/2)}{\sin((\Omega+\Omega_m)/2)} & \text{otherwise} \end{array}\right\}\Bigg|_{N=80}$$

To obtain the multiplied signal $S_{cm}(\Omega)$ expressed by (30), we can calculate the shifted spectral components as follows

$$\frac{1}{4}M(\Omega-2\Omega_c)=\frac{1}{4}\frac{1}{2}[P(\Omega-2\Omega_c+\Omega_m)+P(\Omega-2\Omega_c-\Omega_m)], \quad (32)$$

and

$$\frac{1}{4}M(\Omega+2\Omega_c)=\frac{1}{4}\frac{1}{2}[P(\Omega+2\Omega_c+\Omega_m)+P(\Omega+2\Omega_c-\Omega_m)]. \quad (33)$$

Finally, the spectrum of the signal (30) is expressed as

$$\begin{aligned} S_{cm}(\Omega)&=\frac{1}{4}[P(\Omega-\Omega_m)+P(\Omega+\Omega_m)]+\frac{1}{8}[P(\Omega-2\Omega_c+\Omega_m)+P(\Omega-2\Omega_c-\Omega_m)] \\ &+\frac{1}{8}[P(\Omega+2\Omega_c+\Omega_m)+P(\Omega+2\Omega_c-\Omega_m)] \end{aligned}, \quad (34)$$

and is presented in Figure 14. The power and energy of the signal in the time domain can be calculated from (29) and expressed as

$$\begin{aligned} E_{cm}&=P_{cm}\cdot N=\sum_{n=0}^{N-1}s_{cm}^2(n) \\ &=\sum_{n=0}^{N-1}(\frac{1}{2}A\cos\Omega_m n)^2+\sum_{n=0}^{N-1}(\frac{1}{4}A\cos(2\Omega_c+\Omega_m)n)^2+\sum_{n=0}^{N-1}(\frac{1}{4}A\cos(2\Omega_c-\Omega_m)n)^2 \\ &=\frac{1}{4}\sum_{n=0}^{N-1}\frac{1}{2}A^2+\frac{1}{16}\sum_{n=0}^{N-1}\frac{1}{2}A^2+\frac{1}{16}\sum_{n=0}^{N-1}\frac{1}{2}A^2=\frac{1}{8}A^2N+\frac{1}{32}A^2N+\frac{1}{32}A^2N=\frac{3}{16}A^2N \end{aligned} \quad (35)$$

and the power is $P_{cm}=E_{cm}/N=3A^2/16$. The energy can be calculated in the frequency domain as

$$E_{cm} = \frac{1}{2\pi}\int_{-\pi}^{\pi} |S_{cm}(\Omega)|^2 \, d\Omega$$

$$= \frac{1}{2\pi}\int_{-\pi}^{\pi} |\frac{1}{4}[P(\Omega-\Omega_m)+P(\Omega+\Omega_m)]+\frac{1}{8}[P(\Omega-2\Omega_c+\Omega_m)+P(\Omega-2\Omega_c-\Omega_m)] \quad (36)$$
$$+\frac{1}{8}[P(\Omega+2\Omega_c+\Omega_m)+P(\Omega+2\Omega_c-\Omega_m)]|^2 \, d\Omega$$

$$= 2\frac{A^2}{2\pi}\frac{1}{16}2N\pi + 4\frac{A^2}{2\pi}\frac{1}{64}2N\pi = \frac{3}{16}A^2N$$

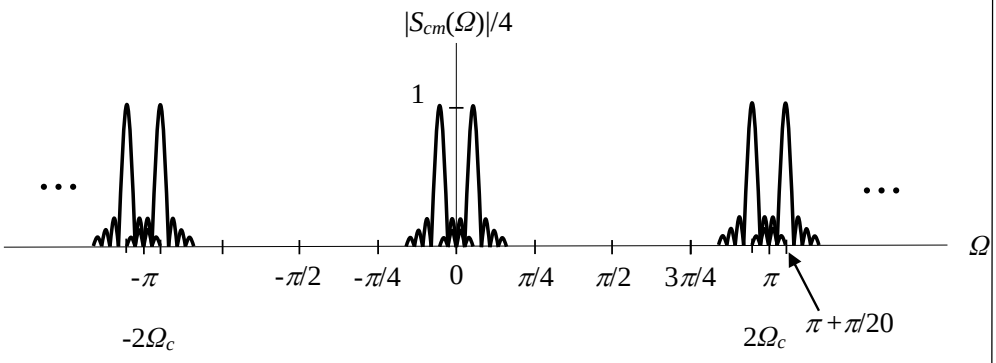

Figure 14 – Magnitude spectral density of the signal at the output of the receiver multiplier
Рис. 14 – Величина спектральной плотности сигнала на выходе приемного умножителя
Слика 14 – Спектрална густина магнитуде сигнала на излазу множача пријемника

Extraction of the baseband rectangular pulse. This extraction starts with a multiplication of the demodulated signal by an LF cosine term as follows

$$s_{mm}(n) = s_{cm}(n)\cos\Omega_m n. \quad (37)$$

Using the modulation theorem, the amplitude spectral density of this signal will be expressed as a shifted version of the spectrum in (34), which gives

Berber, S., Design of a cosine pulse transceiver operating in the discrete-time domain, pp.559-587

$$S_{mm}(\Omega)=\frac{1}{4}P(\Omega)+\frac{1}{8}[P(\Omega-2\Omega_m)+P(\Omega+2\Omega_m)]$$
$$+\frac{1}{4}[P(\Omega-2\Omega_c)+P(\Omega+2\Omega_c)]$$
$$+\frac{1}{8}[P(\Omega-2\Omega_c-2\Omega_m)+P(\Omega-2\Omega_c+2\Omega_m)] \quad , \qquad (38)$$
$$+\frac{1}{8}[P(\Omega+2\Omega_c+2\Omega_m)+P(\Omega+2\Omega_c-2\Omega_m)]$$

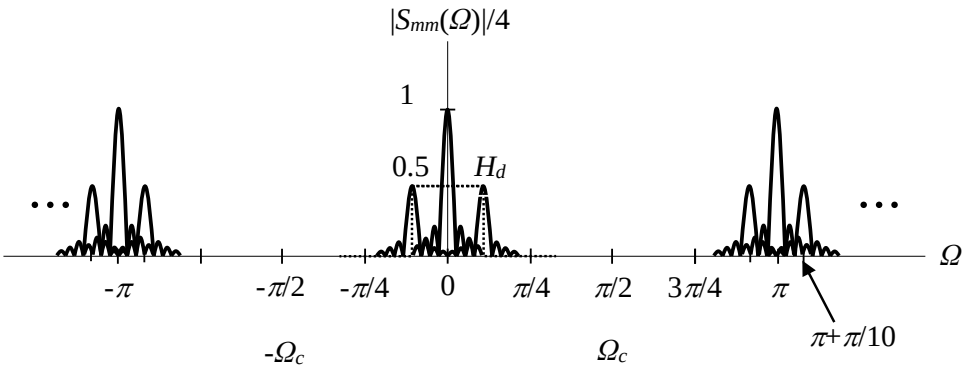

Figure 15 – Magnitude spectral density of $s_{mm}(n)$
Рис. 15 – Спектральная плотность амплитуды сигнала $s_{mm}(n)$
Слика 15 – Спектрална густина магнитуде сигнала $s_{mm}(n)$

The calculated spectrum contains an LF part around the zero frequency, which contains the spectrum of the modulating rectangular pulse. We can use an LP filter to extract this signal. This operation will be approximate, meaning that a part of the spectrum of the neighboring components to the pulse spectrum will be added to the signal causing distortion. Also, the pulse spectrum will be reduced to its two arcades which will reduce the power of the signal. We will take this reduction of the power in the following considerations and calculations.

LPF operation in the time and frequency domain. An ideal LP filter with the gain H_d is used to eliminate the HF components in this spectrum and obtain the demodulated signal representing the rectangular pulse $p(n)$ that was sent by the transmitter. The filter eliminated all high-frequency components and the result is the LF pulse

$$S_{md}(\Omega) = H_d(\Omega) \cdot S_{mm}(\Omega) = H_d(\Omega) \cdot \frac{1}{4} P(\Omega), \qquad (39)$$

where the filter transfer characteristic is rectangular as shown in Figure 15 by a dotted graph of the amplitude H_d. If there is no attenuation of the filter, i.e., H_d =1, an approximation of the output spectrum can be obtained as shown in Figure 16. Due to the limitation of the spectrum of the demodulated pulse $p(n)$ at the receiver side, the received pulse at the output of the LP filter will not be rectangular as the simulation will confirm. In the time domain, the output signal of the filter, $m_d(n)$, will be a convolution of the filter input signal $s_{mm}(n)$ and the impulse response of the filter $h_d(n)$, as will be shown in the simulation. The result of this convolution is the pulse $m_d(n)$, which is a distorted version of the rectangular pulse.

Calculation of the system attenuation. The total value of the demodulated rectangular pulse energy can be calculated from the pulse spectrum in Figure 15, assuming an all-pass LF filter and ideal filtering, as

$$E_{md} = \frac{1}{2\pi} \int_{-\pi}^{\pi} |S_{md}(\Omega)|^2 \, d\Omega = \frac{1}{2\pi} \int_{-\pi}^{\pi} |H_d(\Omega) \cdot \frac{1}{4} P(\Omega)|^2 \, d\Omega$$
$$\underset{H_d=1}{=} \frac{1}{32\pi} \int_{-\pi}^{\pi} |P(\Omega)|^2 \, d\Omega = \frac{A^2}{32\pi} 2N\pi = \frac{1}{18} A^2 N \qquad (40)$$

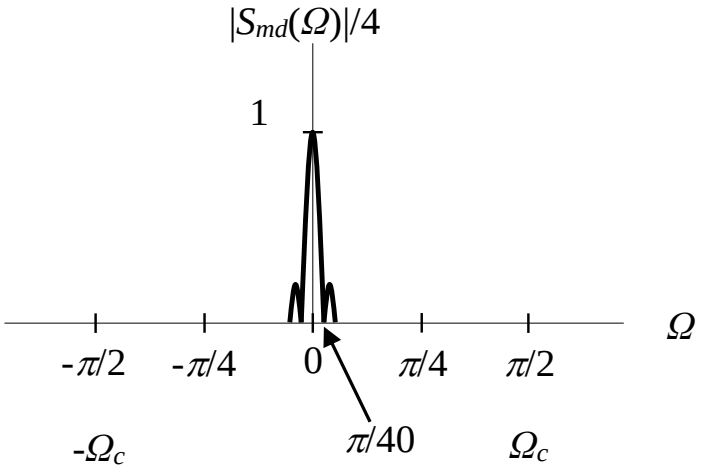

Figure 16 – Magnitude spectral density of the demodulated pulse $m_d(n)$
Рис. 16 – Величина спектральной плотности демодулированного импульса $m_d(n)$
Слика 16 – Спектрална густина магнитуде демодулисаног пулса $m_d(n)$

Berber, S., Design of a cosine pulse transceiver operating in the discrete-time domain, pp.559-587

If we use an LP filter with the cut-off frequency of $\pi/20$, the precise value of the energy of the received pulse is

$$E_{p-Filter} = \frac{1}{32\pi}\int_{-\pi}^{\pi}\left|P(\Omega)\right|^2 d\Omega = \frac{A^2}{32\pi}\int_{-\pi/20}^{\pi/20}\left|\frac{\sin 40\Omega}{\sin(\Omega/2)}\right|^2 d\Omega$$
$$= \frac{A^2}{32\pi}477.5439727897149 = 4.75A^2 = 0.0594NA^2 \quad . \qquad (41)$$

This energy of the signal is much smaller than the energy of the pulse at the transmitter side, which was NA^2, as calculated in (6). The energy of this pulse in its two arcades is

$$E_p = \frac{1}{2\pi}\int_{-\pi}^{\pi}\left|P(\Omega)\right|^2 d\Omega = \frac{A^2}{2\pi}\int_{-\pi/20}^{\pi/20}\left|\frac{\sin 40\Omega}{\sin(\Omega/2)}\right|^2 d\Omega = \frac{A^2}{2\pi}2N\pi$$
$$= \frac{A^2}{2\pi}477.5439727897149 = 76A^2 = 0.95NA^2 \quad . \qquad (42)$$

The power attenuation of the received signal is

$$a_p = 10\log_{10}\frac{P_p}{P_{p-filter}} = 10\log_{10}\frac{E_p/N}{E_{p-filter}/N} = 10\log_{10}\frac{0.95A^2}{0.0594A^2} = 12.04\,\text{dB}. \qquad (43)$$

To receive the pulse with the required power, we need to use amplifiers in the receiver. These amplifiers will compensate for the loss of power caused by the explained signal processing. However, due to the propagation of the signal, there will exist additional attenuation that needs to be compensated by the amplification inside the receiver. Finally, as shown in Figure 1, there will be a noise present in the channel that is added to the signal. The noise influence on the signal transmission needs to be also considered, which is a separate problem in the analysis of the system.

If we are interested in the detection of the phase of the transmitted cosine pulse, we can use a correlator on the receiver side. In that case, the polarity of the correlator output will give us evidence about the phase of the transmitted pulse.

Simulation of the receiver

The receiver operation is simulated in Matlab. The simulated operation of the first modulation multiplier is presented by the graphs of its output discrete-time signal $s_{cm}(n)$ in the time and frequency domain in Figure 17, which was theoretically analyzed and presented in the frequency domain in Figure 14.

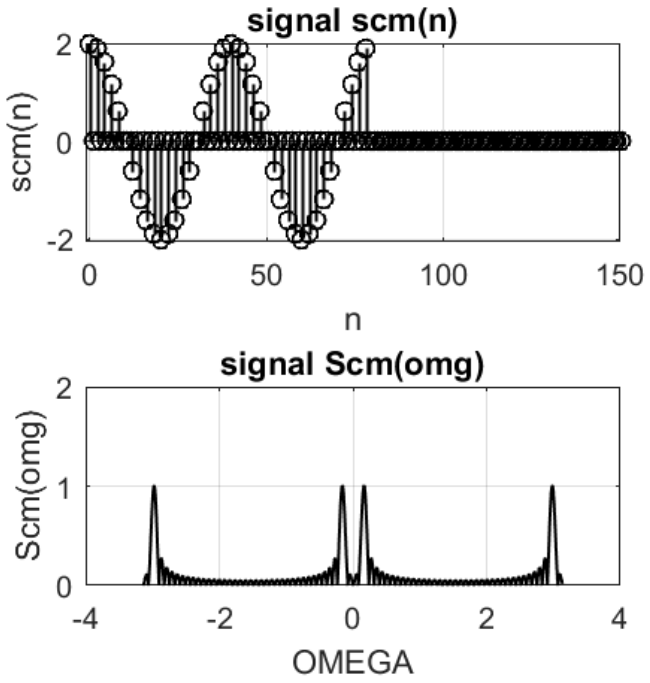

Figure 17 – Magnitude spectral density of the simulated signal at the output of the receiver multiplier
Рис. 17 – Величина спектральной плотности моделируемого сигнала на выходе умножителя приемника
Слика 17 – Спектрална густина магнитуде симулисаног сигнала на излазу множача пријемника

This signal is multiplied by an LF signal $s_m(n)$ to get the signal $s_{mm}(n)$ that contains a low-frequency component that represents the modulating signal. The simulated signal in the time and frequency domain is shown in Figure 18. The corresponding signal, theoretically calculated, is presented in Figure 15.

Berber, S., Design of a cosine pulse transceiver operating in the discrete-time domain, pp.559-587

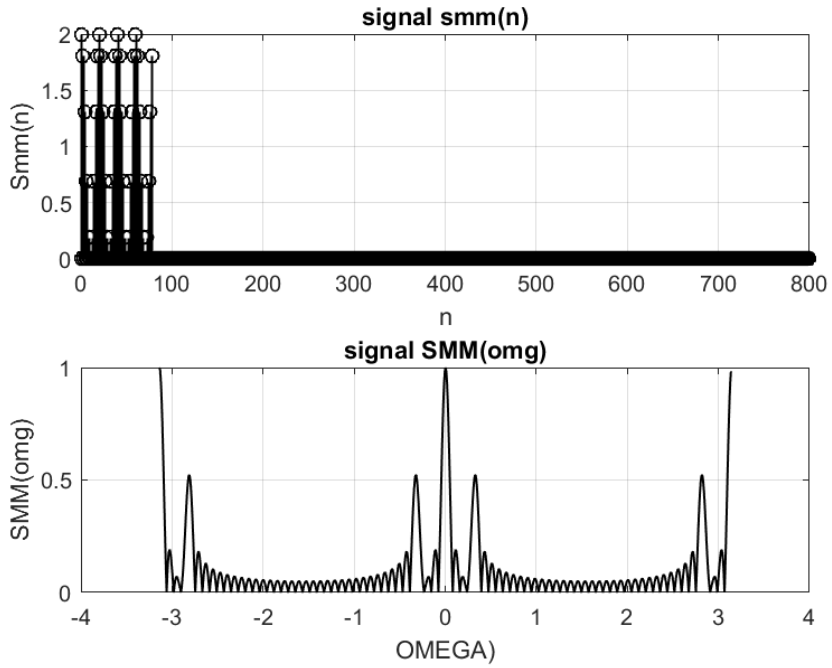

Figure 18 – Magnitude spectral density of the simulated $s_{mm}(n)$
Рис. 18 – Спектральная плотность моделируемой величины $s_{mm}(n)$
Слика 18 – Спектрална густина магнитуде симулисаног $s_{mm}(n)$

The LF signal $s_{mm}(n)$ is processed in the LP filter to get the LF modulating signal. For the filter transfer characteristic shown in Figure 14, the impulse response $h_d(n)$ is calculated.

Then the convolution of this impulse response and the input signal $s_{mm}(n)$ is performed in the time domain as shown in Figure 19.

The LPF is a linear time-invariant discrete-time system, and this convolution can be performed.

The result of the convolution is the positive pulse $m_d(n)$ that is generated at the output of the receiver and corresponds to the rectangular pulse sent at the transmitter side.

This pulse obtained by simulation is presented in Figure 20.

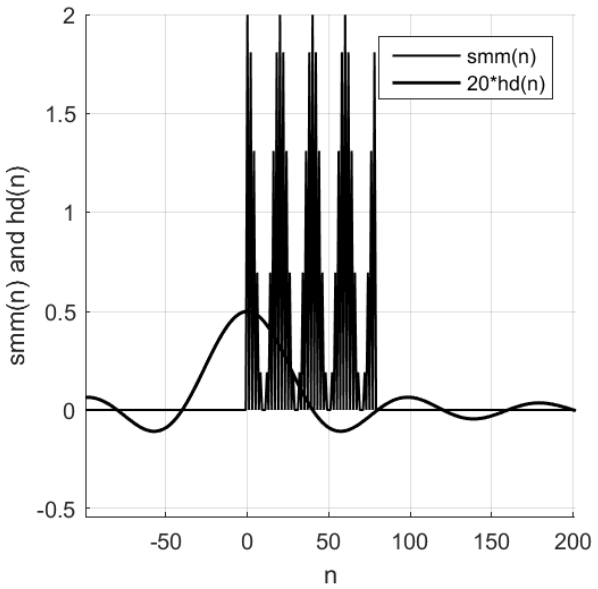

Figure 19 – Procedure of convolution to get the demodulated pulse $m_d(n)$
Рис. 19 – Процедура свертки для получения демодулированного импульса $m_d(n)$
Слика 19 – Процедура конволуције за добијање демодулисаног пулса $m_d(n)$

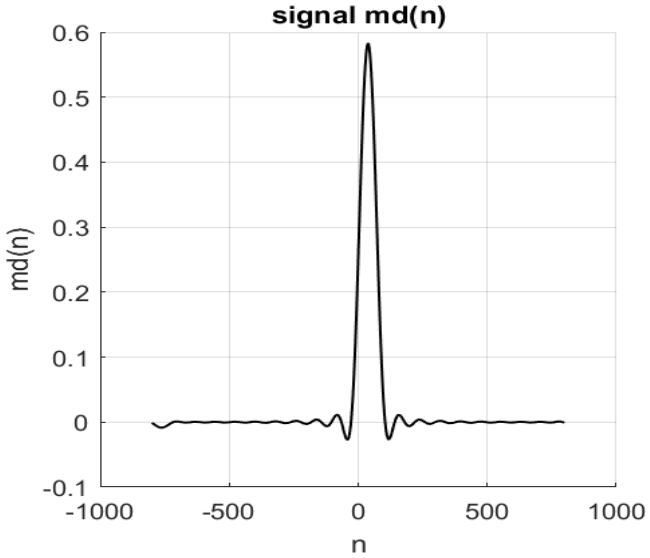

Figure 20 – The demodulated pulse $m_d(n)$ at the output of the LP filter
Рис. 20 – Демодулированный импульс $m_d(n)$ на выходе фильтра нижних частот
Слика 20 – Демодулисани пулс $m_d(n)$ на излазу НФ филтера

Conclusions

This paper presented the theoretical model and the simulation results of a communication system analysis for a cosine pulse transmission. A detailed block schematic of the system's transmitter and receiver is presented in the form of mathematical operators and all input-output signals are presented in both time and frequency domains using exact mathematical expressions. To calculate the attenuation of the signals in the system, the powers and the energies of the signals are calculated for all signals processed in the system.

It is shown that the application of a low-pass filter inside the receiver allows the detection of the modulating signal, despite its distortion due to the processing in the system. The signals in the analyzed blocks of the transceiver are processed in the discrete-time domain. All theoretical results are confirmed by simulations.

References

Abramowitz, M. & Stegun, I.A. 1972. *Handbook of Mathematical Functions with Formulas, Graphs, and Mathematical Tables.* Washington, D.C.: United States Department Of Commerce, National Bureau of Standards, Applied Mathematics Series – 55 [online]. Available at: https://personal.math.ubc.ca/~cbm/aands/frameindex.htm [Accessed: 20 March 2023].

Benvenuto, N., Corvaja, R., Erseghe, T. & Laurenti, N. 2007. *Communication Systems, Fundamentals and Design Methods*. Hoboken, NJ, USA: John Wiley & Sons, Inc. ISBN-13: 978-0470018224.

Berber, S. 2009. *Deterministic and Stochastic Signal Processing: Continuous and Discrete-time Signals.* VDM Verlag Dr. Müller. ISBN-13: 978-3639111880.

Berber, S. 2019. Discrete time domain analysis of chaos-based wireless communication systems with imperfect sequence synchronization. *Signal Processing*, 154, pp.198-206. Available at: https://doi.org/10.1016/j.sigpro.2018.09.010.

Berber, S. 2021. *Discrete Communication Systems*. Oxford, UK: Oxford University Press. ISBN-13: 978-0198860792.

Cavicchi, T.J. 2000. *Digital Signal Processing, Solutions Manual.* Hoboken, NJ, USA: John Wiley & Sons, Inc. [Accessed: 20 March 2023].

Haykin, S. 2014. *Digital Communication Systems, 1st edition.* Hoboken, NJ, USA: John Wiley & Sons, Inc. ISBN-13: 978-0-471-64735-5.

Ingle, V.K. & Proakis, J.G. 2012. *Digital signal processing using MATLAB*, *3rd edition*. Stamford, CT, USA: Cengage Learning. ISBN-13: 978-1-111-42737-5.

-Integral calculator. 2023. *Calculate integrals online − with steps and graphing!* [online]. Available at: https://www.integral-calculator.com [Accessed: 20 March 2023].

Manolakis, D.G., Ingle, V.K. & Kogan, S.M. 2005. *Statistical and Adaptive Signal Processing: Spectral Estimation, Signal Modeling, Adaptive Filtering and Array Processing, Illustrated edition*. Norwood, MA, USA: Artech House. ISBN-13: 978-1580536103.

Miao, G.J. 2007. *Signal Processing in Digital Communications*. Norwood, MA, USA: Artech House. ISBN 13: 978-1-58053-667-7.

Nguyen, X.Q, Vu, V.Y. & Trung, Q.D. 2015. Design and analysis of a spread-spectrum communication system with chaos-based variation of both phase-coded carrier and spreading factor. *IET Commun*., 9(12), pp.1466-1473. Available at: https://doi.org/10.1049/iet-com.2014.0907.

Papoulis, A. & Pillai, S.U. 2002. *Probability, Random Variables, and Stochastic Processes, 4th edition.* McGraw-Hill Europe. ISBN-13: 978-0071226615.

Proakis, J.G. 2001. *Digital Communications, 4th edition.* McGraw Hill Higher Education. ISBN-13: 978-0071181839.

Rice, M. 2009. *Digital Communications: A Discrete-time Approach*, *1st edition*. London, UK: Pearson Prentice Hall. ISBN-13: 978-0130304971.

Разработка приемопередатчика косинусоидальных импульсов в дискретном времени

Стеван М. Бербер

Университет Окленда,
Кафедра электротехники, вычислительной техники и программного обеспечения, г. Окленд, Новая Зеландия

РУБРИКА ГРНТИ: 50.07.03 Теория и моделирование вычислительных сред, систем, комплексов и сетей
ВИД СТАТЬИ: оригинальная научная статья

Резюме:

Введение/цель: В данной статье обсуждаются вопросы теории и разработки приемопередатчика для передачи косинусоидальных импульсов в дискретном времени. Работа приемопередатчика и все сигналы анализируются как во временной, так и в частотной областях.

Методы: В данной статье приведен подробный обзор теоретических моделей приемопередатчика на основе его блок-схем, которые представлены с помощью математических операторов. Результаты смоделированных блоков приемопередатчика были сопоставлены с результатами теоретического анализа.

Результаты: Сигналы дискретного времени на входах и выходах каждого блока приемопередатчика выводятся в математической форме и отображаются во временной и частотной областях. Симулятор приемопередатчика был разработан в Matlab. Теоретические выводы подтверждены результатами моделирования.

Выводы: Результаты данной статьи способствуют теоретическому моделированию и разработке современных примоередатчиков, которые можно будет использовать для передачи дискретного косинусоидального импульса.

Ключевые слова: разработка приемопередатчика, дискретный косинусоидальный импульс, импульсный приемопередатчик, математическое моделирование приемопередатчика, фильтрация, симулятор приемопередатчика.

Дизајн примопредајника косинусног пулса у дискретном времену

Стеван М. Бербер

Универзитет у Окланду,
Катедра за електротехнику, рачунарску и софтверску технику,
Окланд, Нови Зеланд

ОБЛАСТ: електротехника, телекомуникације
КАТЕГОРИЈА (ТИП) ЧЛАНКА: оригинални научни рад

Сажетак:

Увод/циљ: Дизајн примопредајника косинусног пулса приказан је у дискретном времену. Рад примопредајника и сви сигнали анализирани су у временском и фреквенцијском домену.

Методе: Приказани су детаљни теоријски модели предајника и пријемника базирани на њиховим блок-шемама које су представљене помоћу математичких оператора. Блокови примопредајника су симулирани, а резултати симулације упоређени са резултатима теоријске анализе.

Резултати: Сигнали дискретног времена на улазима и излазима сваког блока у примопредајнику изведени су у математичком облику и приказани у временском и фреквенцијском домену. Развијен је симулатор примопредајника у Матлаб-у. Резултати симулације су потврдили теоријске налазе.

Закључак: Резултати овог рада доприносе теоријском моделовању и дизајну модерних приморедајника који се могу користити за пренос дискретног косинусног пулса.

Кључне речи: дизајн примопредајника, дискретни косинусни пулс, примопредајник пулса, математичко моделовање примопредајника, филтрирање, симулатор примопредајника.

Paper received on / Дата получения работы / Датум пријема чланка: 23.03.2023.
Manuscript corrections submitted on / Дата получения исправленной версии работы / Датум достављања исправки рукописа: 12.06.2023.
Paper accepted for publishing on / Дата окончательного согласования работы / Датум коначног прихватања чланка за објављивање: 14.06.2023.

© 2023 The Author. Published by Vojnotehnički glasnik / Military Technical Courier (www.vtg.mod.gov.rs, втг.мо.упр.срб). This article is an open access article distributed under the terms and conditions of the Creative Commons Attribution license (http://creativecommons.org/licenses/by/3.0/rs/).

© 2023 Автор. Опубликовано в «Военно-технический вестник / Vojnotehnički glasnik / Military Technical Courier» (www.vtg.mod.gov.rs, втг.мо.упр.срб). Данная статья в открытом доступе и распространяется в соответствии с лицензией «Creative Commons» (http://creativecommons.org/licenses/by/3.0/rs/).

© 2023 Аутор. Објавио Војнотехнички гласник / Vojnotehnički glasnik / Military Technical Courier (www.vtg.mod.gov.rs, втг.мо.упр.срб). Ово је чланак отвореног приступа и дистрибуира се у складу са Creative Commons лиценцом (http://creativecommons.org/licenses/by/3.0/rs/).